Heliyon 9 (2023) e18811

Contents lists available at ScienceDirect

Heliyon

journal homepage: www.cell.com/heliyon

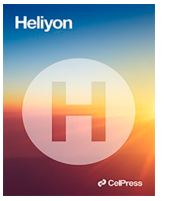

Structural analysis and characterization of date palm fiber-based low-cost carbon nanotubes and nanostructured powder activated carbon

Alfarooq O. Basheer [a], Ali Abu Odeh [b], Y. Al-Douri [c,d,e,f,*]

[a] Department for Earth Sciences and Environment, Faculty of Science and Technology, Universiti Kebangsaan Malaysia, 43600, Bangi, Selangor, Malaysia
[b] Academic Support Department, Abu Dhabi Polytechnic, P.O. Box 111499, Al Ain, United Arab Emirates
[c] Nanotechnology and Catalysis Research Centre, University of Malaya, 50603, Kuala Lumpur, Malaysia
[d] Department of Applied Physics and Astronomy, College of Sciences, University of Sharjah, P.O. Box 27272, Sharjah, United Arab Emirates
[e] Department of Mechanical Engineering, Faculty of Engineering, Piri Reis University, Eflatun Sk. No:8, 34940, Tuzla, Istanbul, Turkey
[f] Department of Physics, Faculty of Science, Sana'a University, Sana'a, Yemen

ARTICLE INFO

Keywords:
Biomass
Carbon nanotubes
Structural

ABSTRACT

The structural properties and characteristics of date palm fiber-based low-cost carbon nanotubes (CNTs) and nanostructured powder activated carbon (DP-NPAC) are investigated. The DP-NPAC and CNTs are prepared using an environmentally friendly method, and characterized and analyzed using field emission-scanning electron microscopy (FESEM), transmission electron microscopy (TEM), and X-ray diffraction (XRD). The results have showed that both DP-NPAC and CNTs possess crystallite structure, nano-scale, high capacity, cost-effective for multi-application that make them efficient for future fabrication and manufacturing. It is supposed that DP-NPAC biomass is to be used as potential and cost-effective precursor for synthesized CNTs.

1. Introduction

The critical environmental issues have a global effect due to its harmful impact on human health and ecosystem [1]. Some of them causes various health problems like Alzheimer's disease, kidney damage and bone disorders [2,3]. However, the production of activated carbon (AC) from conventional raw materials as coconut shells and coal, is costly and not environmentally friendly. Therefore, there is a necessity to explore sustainable raw materials and low-cost for producing AC [4]. The nanotechnology has emerged as a promising field for developing new materials with unique properties and applications. Carbon nanotubes (CNTs) are one of the most promising nanomaterials due to their excellent mechanical, electrical and thermal properties. However, the high cost of CNTs limits their widespread usage [5–7]. Therefore, there has been a growing interest in exploring alternative sustainable raw materials and cost-effective for producing AC. Date palm fiber is a sustainable raw material and low-cost that has the potential to be used as a precursor for activated carbon, in turn it is a precursor for carbon nanotubes (CNTs) that are another promising material for potential application due to its unique physical and chemical properties because they have high surface area, high mechanical strength and chemical stability [8].

* Corresponding author. Nanotechnology and Catalysis Research Centre, University of Malaya, 50603, Kuala Lumpur, Malaysia.
E-mail address: yaldouri@yahoo.com (Y. Al-Douri).

https://doi.org/10.1016/j.heliyon.2023.e18811
Received 22 June 2023; Received in revised form 27 July 2023; Accepted 28 July 2023
Available online 31 July 2023

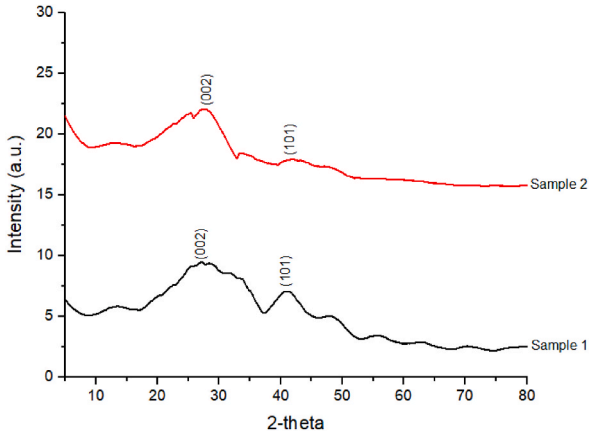

Figure [1]. XRD scheme of 1) I-PAC and sample 2) I-CNT.

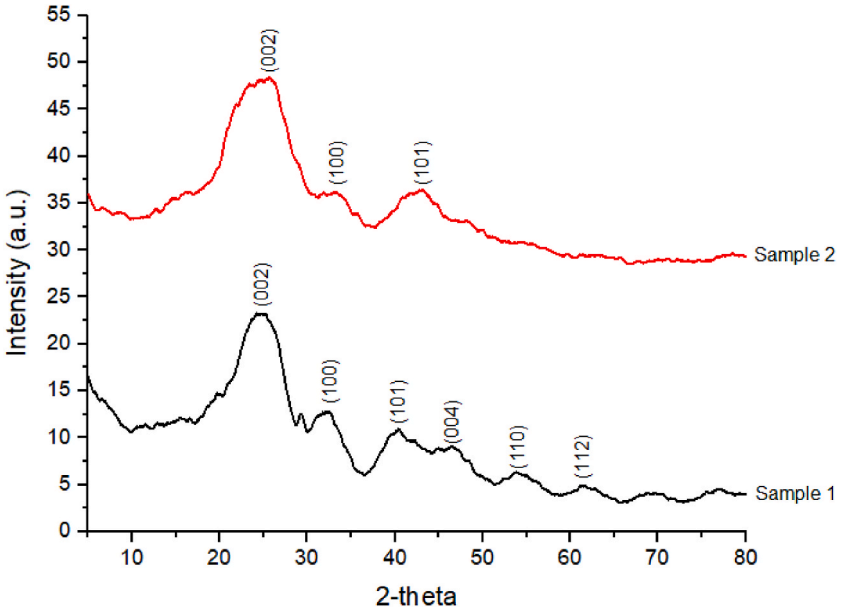

Figure [2]. XRD scheme of 1) O-PAC and sample 2) O-CNT.

Table 1
The structural properties of activated carbon, 1) I-PAC and sample 2) I-CNT.

Sample	2θ	D (nm)	FWHM	*hkl*	d (Å)	a and c (Å)	ε	δ (10^{14} lines/m^2)
1	29.39	55.87	0.147	002	3.04	a = 3.72, c = 6.07	0.035	3.2
2	29.37	27.25	0.323	002	3.04	a = 3.73, c = 6.07	0.078	15.4

Table 2
The structural properties of carbon nanotubes, 1) O-PAC and sample 2) O-CNT.

Sample	2θ	D (nm)	FWHM	*hkl*	d (Å)	a and c (Å)	ε	δ (10^{14} lines/m^2)
1	24.31	110.27	0.073	002	3.66	a = 4.48, c = 7.31	0.018	0.82
2	24.48	55.3	0.147	002	3.63	a = 4.45, c = 7.26	0.036	3.27

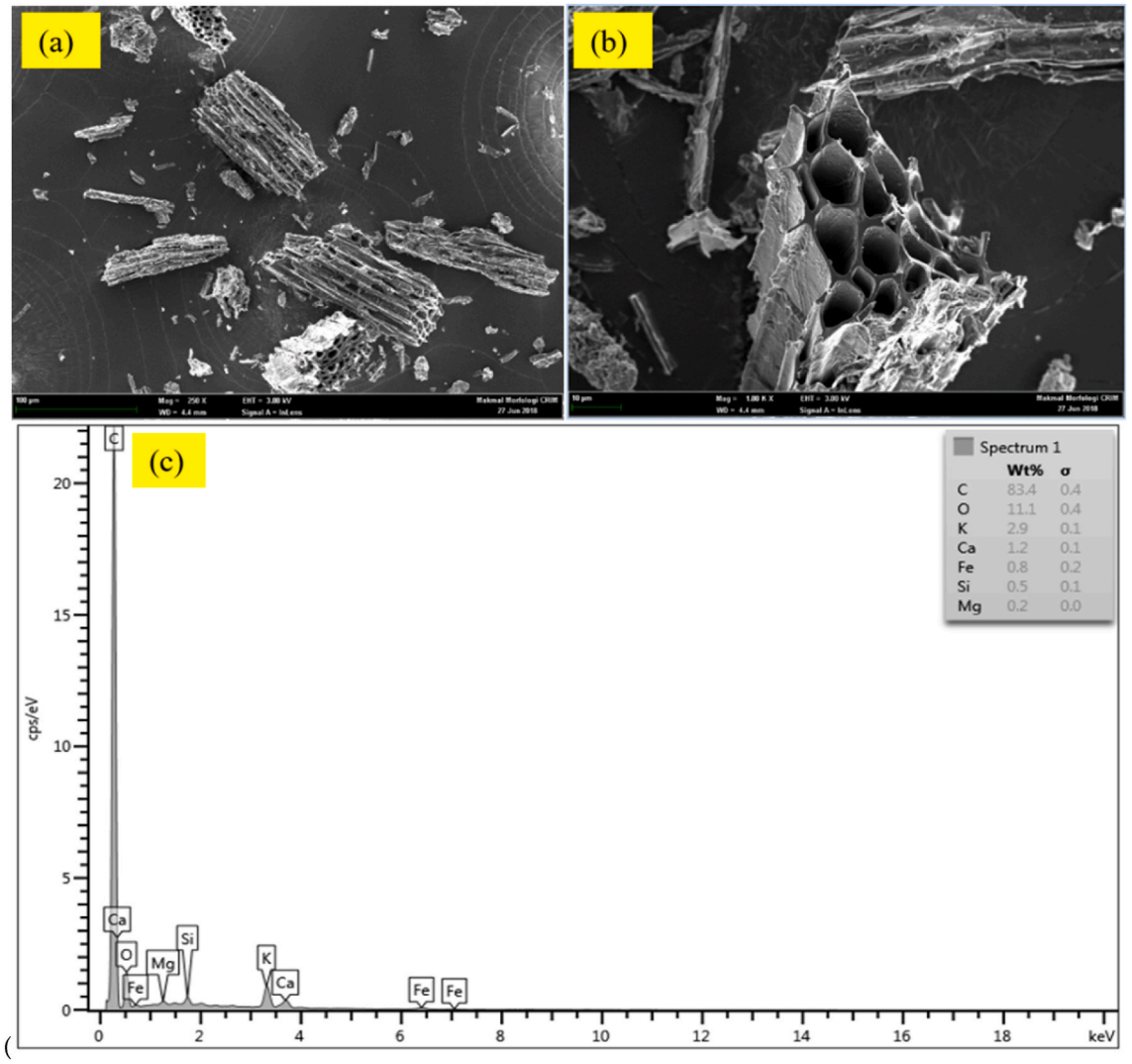

Figure [3]. (a,b) FESEM of different magnifications for I-PAC, (c) EDX.

Recently, Gao et al. [9] have utilized aluminum to promote the aluminum-water reaction to continue efficiently, the reaction needs to be activated. Continuous reactions are difficult to be achieved at high temperature and pressure, where it becomes a difficult to obtain reaction initiation and development processes. They have investigated aluminum-water reaction process at medium temperature using micron aluminum powder. While. Da et al. [10] have introduced the nitrogen-rich porous carbon to fabricate novel N-rich graphite supported aluminum composite. They have presented nitrogen-rich porous carbon to make Al-Gr contain plentiful N species and improve physiochemical property of Al-Gr. Otherside, Morovvati et al. [11] have used chemical vapor deposition (CVD) to synthesize CNTs on aluminum (Al) substrate for evaluating the fracture initiation and damage progression in Al-CNT composites. They have researched the mechanical and materials properties in CNTs to explore the importance of microstructural process in fracture of ductile and stress effect on growth rate. And, Liu et al. [12] have characterized arsenic (As) in flue gas (FG) that is prepared by plants of coal power at different temperatures via thermodynamics computations and density functional theory (DFT). They have investigated interaction of gaseous species of As with AlN CNTs.

In this work, the novelty is to synthesize biomass-based new cost-effective nanomaterial focused on structural analysis, characterization and surface morphology through X-ray diffraction (XRD), field emission-scanning electron microscopy (FESEM) and transmission electron microscopy (TEM). To the best of our knowledge, there is no other study available in the literature. We have investigated the structural properties of using date palm fiber-based low-cost carbon nanotubes (CNTs) and nanostructured powder activated carbon (DP-NPAC). Date palm fibers are abundant as agricultural waste material and low-cost that have been used in multi-application as paper production, animal feed and building materials. The combination of date palm fibers with nanotechnology has the potential to produce sustainable adsorbent material and low-cost. The aim of this study is to characterize the structural properties of DP-NPAC and CNTs and evaluate their potential performance for multi-application. This work is divided as the followings; section 2

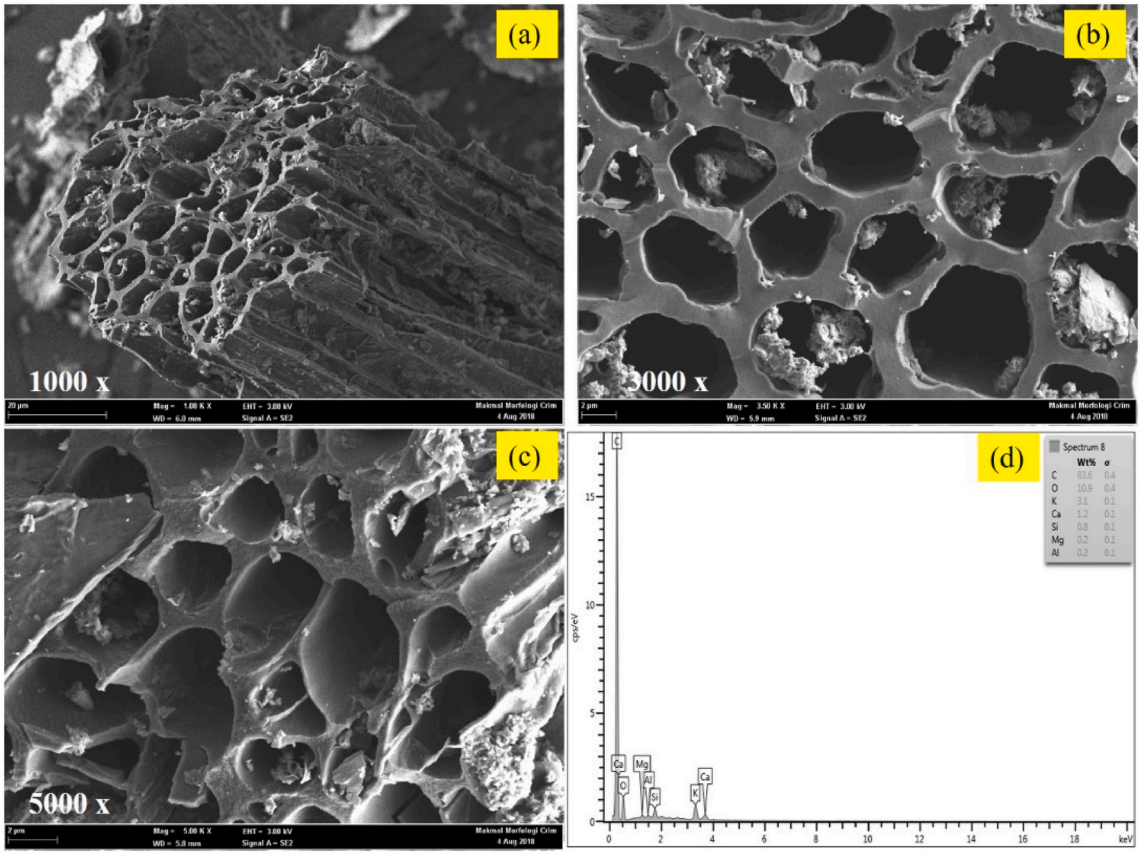

Figure [4]. FESEM for different magnifications for O-PAC (a, b and c) and EDX (d) of NPAC.

details the experimental procedure, followed by section 3 to elaborate results and discussion. And, section 4 is outlined the conclusions.

2. Experimental

The date palm fibers are collected from two different countries, Iraq and Oman's date palm farms and washed with distilled water to remove any impurities. For synthesizing nanostructured powder activated carbon (DP-NPAC) utilizing date palm fiber, the date palm fibers are first pyrolyzed at 500 °C for 2 h in a muffle furnace to produce biochar. The biochar is then activated by chemical treatment with potassium hydroxide (KOH) at a mass ratio of 1:4 (biochar:KOH) at 700 °C for 1 h. The resulted activated carbon is then ground into a fine powder (DP-NPAC) using a ball mill. While, for synthesizing low-cost carbon nanotubes (CNTs), the CNTs are synthesized by chemical vapor deposition (CVD) utilizing acetylene gas as a source of carbon and iron nanoparticles like a catalyst. The CNTs are purified by acid treatment with a mixture of hydrochloric acid and nitric acid to remove any residual impurities.

2.1. Growth of CNTs production on DP-NPAC

Fe $(NO_3)_3.9H_2O$, acetone, C_2H_2, H_2 and N_2 are used for CNTs growth. Ultra-sonication and (CVD) equipment's have been utilized for fabrication as well. Iron (Fe) catalyst is selected for synthesizing CNTs. The elementary preparation method is wetness impregnation by sonication. Fe (NO_3) added in 5 ml acetone, then mixed with 2 g PAC. However, mixture is sonicated at 60 °C for 99 min till acetone evaporated. Subsequently sample DP-NPAC/Fe is dried overnight at 105 °C. Therefore, calcined DP-NPAC/Fe at 400 °C at 2 h under inert gas purified N_2, 200 ml/min, then cooled and stored to be used in CNTs production. Furthermore, the system is initially flushed with N_2 in order to ensure an oxygen free environment. The calcined sample (300 mg PAC/Fe) is placed in a ceramic alumina boat into CVD reactor chamber. The growth is carried out under H_2 at 550 °C with flow rates of 160 ml/min, followed by C_2H_2 mixing with H2 1:4 ratio and passing through a heated reactor for 47 min. After growing CNTs and cooling the sample to room temperature with a purified N_2 flow rate of 200 ml/min, the synthesized CNTs are collected and weighted.

The structural properties of DP-NPAC and CNTs are analyzed and characterized by different techniques such as X-ray diffraction (XRD) (PerkinElmer, USA), transmission electron microscopy (TEM) (JEOL 2000FX, UK) and field emission-scanning electron microscopy (FESEM) (model ZEISS Merlin, UK). The materials and method used in this work provide a comprehensive approach to the

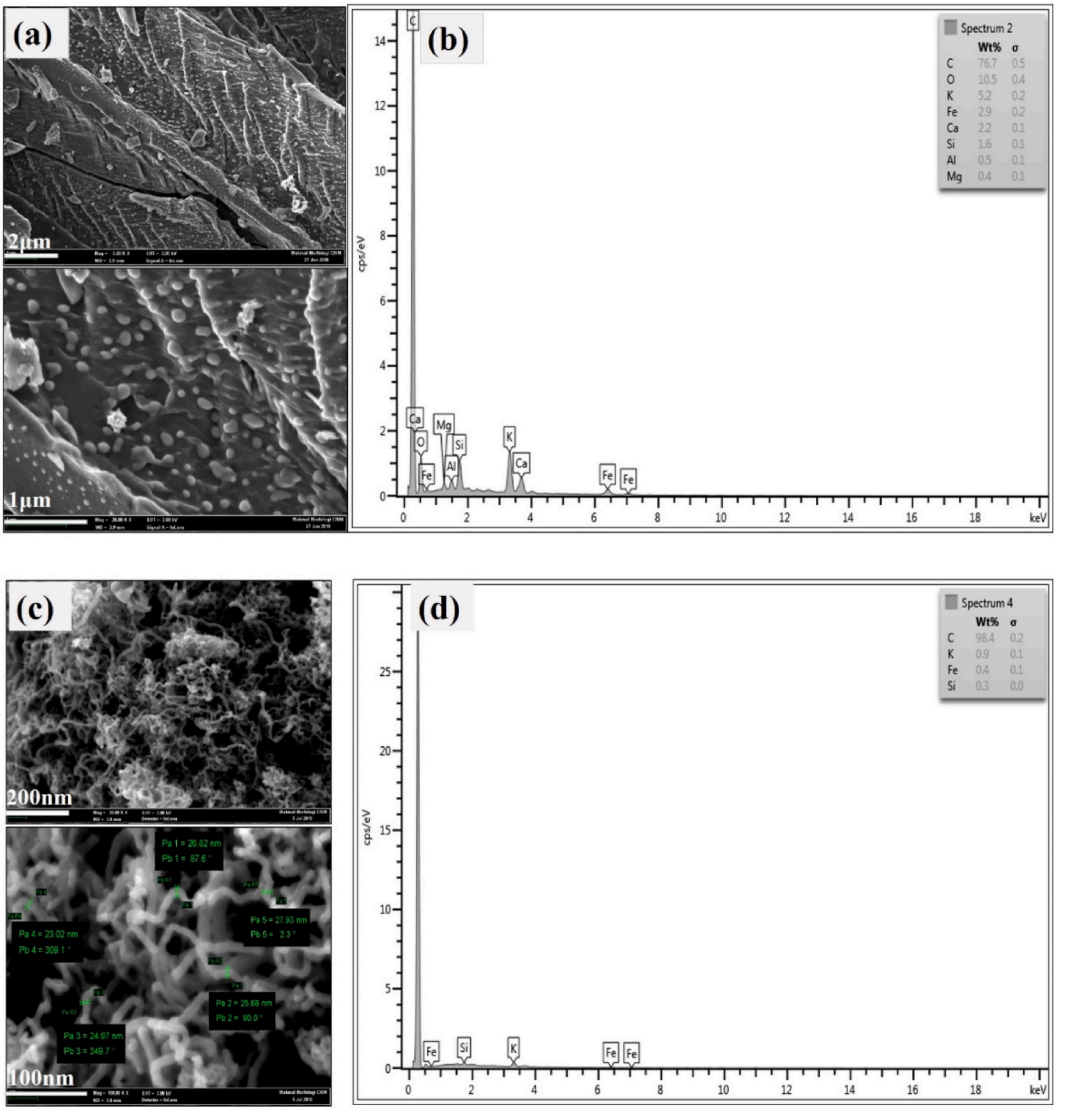

Figure [5]. (a) FESEM; (b) EDX of I-CNT with Fe catalyst before growth, while (c) FESEM and (d) EDX for I-CNT after growth.

synthesis and characterization of DP-NPAC and CNTs.

3. Results and discussion

To evaluate the carbon staking structure, it is understood for using X-ray diffraction (XRD) [13]. Figures [1,2] illustrate the XRD patterns of Iraqi powder activated carbon (I-PAC), Iraqi carbon nanotube (I-CNT), Omani powder activated carbon (O-PAC) and Omani carbon nanotube (O-CNT), respectively for an optimum condition. The date palm fiber (DPF) has amorphous structure that corresponding to the high degree of content for lignin and hemicellulose [14]. To reduce the amorphous structure, it is noticed during the conversion process of Omani date palm fiber (O-DPF) and Iraqi date palm fiber (I-DPF) to NPAC, the lignin and hemicellulose are uncovered to high temperatures [15]. Furthermore, the highest peaks at 27.33° and 41.29°, 27.53° and 43.90° that are attributed to (002) and (101) for I-CNT and O-CNT, respectively are illustrated a partially structure of CNT [16]. The distance of inter-planer (d) is computed utilizing Bragg's law;

$$d = \frac{n\lambda}{2\,sin(\theta)} \quad [1]$$

where $\lambda = 1.5406$ Å refers to XRD wavelength and Bragg's angle refers to θ. The hexagonal structure has lattice constants a and c that are computed of XRD using the formulas below;

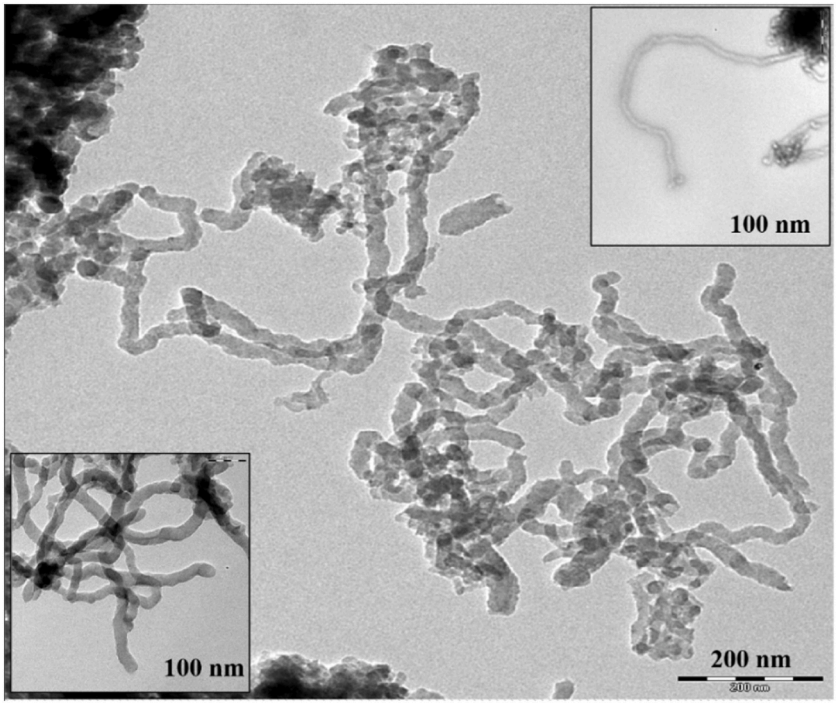

Figure [6]. Tem for I-CNT.

$$\frac{1}{d^2}=\frac{4}{3}\left(\frac{h+hk+k^2}{a^2}\right)+\frac{l}{c^2} \quad [2]$$

$$\frac{c}{a}=1.63 \quad [3]$$

D refers to crystallite size that is extracted by Scherrer's formula;

$$D=\frac{k\,\lambda}{\beta\,cos(\theta)} \quad [4]$$

where $k=0.9$, and full width at half maximum (FWHM) for diffraction peaks in radian refers to β. The strain (ε) and dislocation density (δ) for plane (002) are displayed in Tables 1 and 2, which are computed via the followings;

$$\delta=\frac{1}{D^2} \quad [5]$$

$$\varepsilon=\frac{\beta\,cos\,\theta}{4} \quad [6]$$

The crystallite size for I-PAC and I-CNT is smaller than for O-PAC and O-CNT in corresponding with inter-planer distance, lattice constants and contrary to strain and dislocation density, which reflects the optimum case for multi-field application.

Field emission scanning electron microscopy (FESEM) is employed to examine the surface morphology of NPAC for an optimum condition. FESEM and EDX are shown in Fig. [3] for investigating I-PAC's morphology that is prepared from an optimum condition for DPF. Fig. [3(a, b)] illustrates fairly and harmonious similar affiliation with arranged pores. It is indicated that the tubes form pore structure of synthesized I-PAC. Moreover, it is known that formulation of developed pores high surface area on fiber surface can be firmly reached through activating agent along with activation procedure. Fig. [3c] illustrates elements composition of I-PAC utilizing EDX spectroscopy. Moreover, EDX has confirmed NPAC element makeup of 83.4 C (wt %), 1.1 O (wt %), 2.9 K (wt %), 1.2 Ca (wt %), 0.8 Fe (wt %), 0.5 Si (wt %), and 0.2 Mg (wt %).

The EDX analysis and FESEM images at varied magnifications of O-PAC are shown in Fig. [4]. The O-DPF-based NPAC has to demonstrate a homogeneous distribution of pore size including a uniform arrangement of pores that are available on NPAC EDX analysis in honey-comb structure and well-arranged forms. The same trends are available in previous studies [17–19]. Fig. [4] has shown that NPAC has large surface area applicable to adsorption of water pollutants. While, Nasrullah et al. [20] have found a deep relevance between surface areas of adsorbents. Moreover, EDX has confirmed NPAC elements for 83.6 C (wt %), 10.9 O (wt %), 3.1 K (wt %), 1.2 Ca (wt %), 0.8 Si (wt %), 0.2 Mg (wt %), and 0.2 Al (wt %).

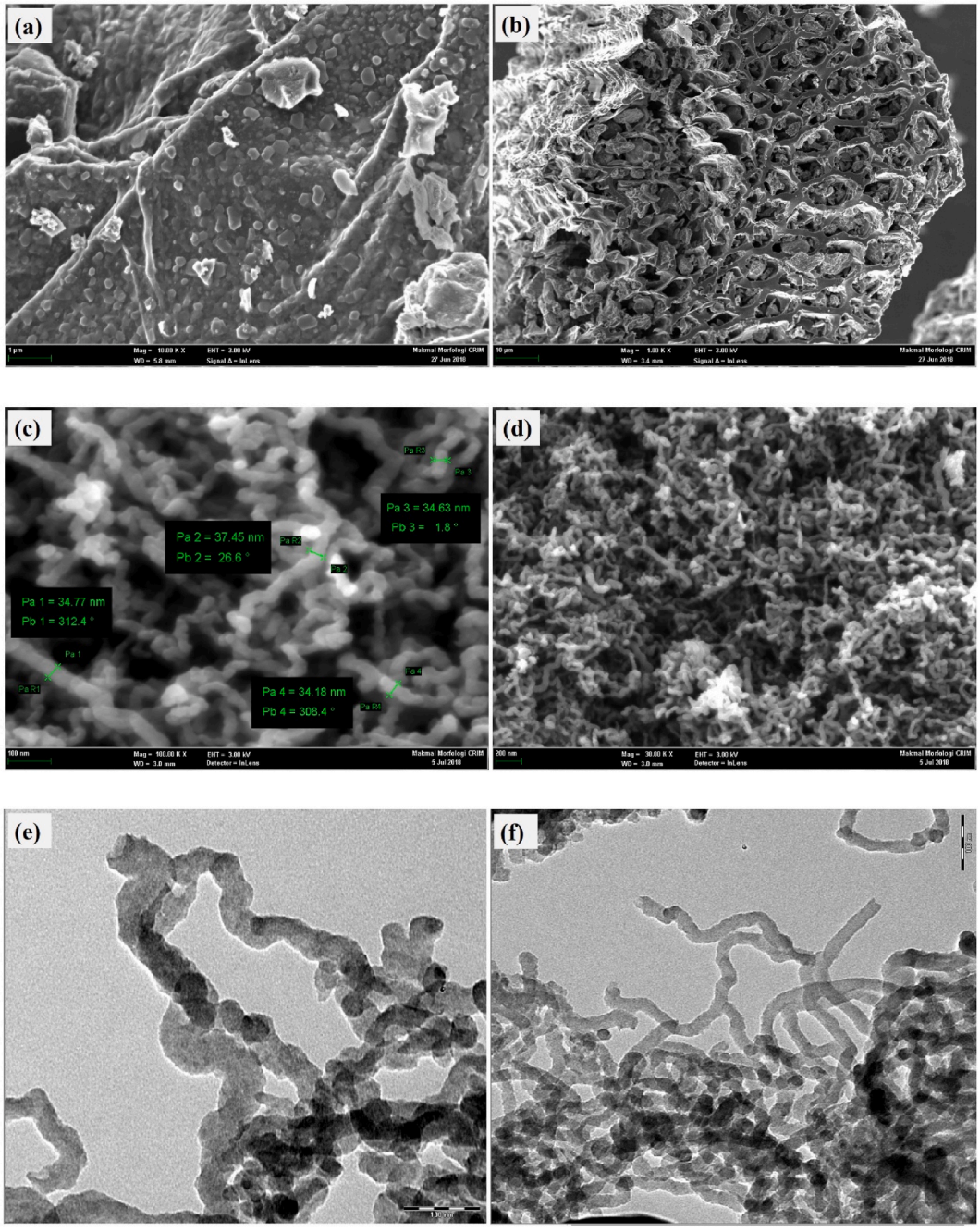

Figure [7]. FESEM (a,b) before growth, (c,d) O-CNT and TEM (e,f) of O-CNT.

To investigate the morphology and surface structure of synthesized materials, including date palm fiber-based low-cost carbon nanotubes (CNTs) and nanostructured powder activated carbon (DP-NPAC). FESEM uses electronic focused beam for scanning sample surface to generate high-resolution images of its topography and surface features. FESEM provides information on the size, shape and distribution of particles, as well as presence of pores and other structural features.

Fig. [5a] shows a rough surface before growth for I-CNT/Fe within dispersion of Fe catalyst. After decomposition of C_2H_2, I-CNT shows agglomeration and network for CNTs grown on I-PAC to provide robust proof for Fe catalyst of growth of CNTs as illustrated in Fig. [5c]. So, diameter of I-CNT is about 23.02–27.93 nm. Furthermore, the unique growth of CNTs is attributed to bottom of Fe, and entire Fe particle pushed off I-PAC to indicate growth model of "base or root". The weak interaction of I-PAC and Fe is attributed to physical adsorption on I-PAC [21,22]. Furthermore, for determining materials' elements before and after growth, it is necessary to use EDX. The EDX of I-PAC/Fe and I-CNT is shown in Fig. [5(b, d)], respectively. The successful impregnated on I-PAC is illustrated in

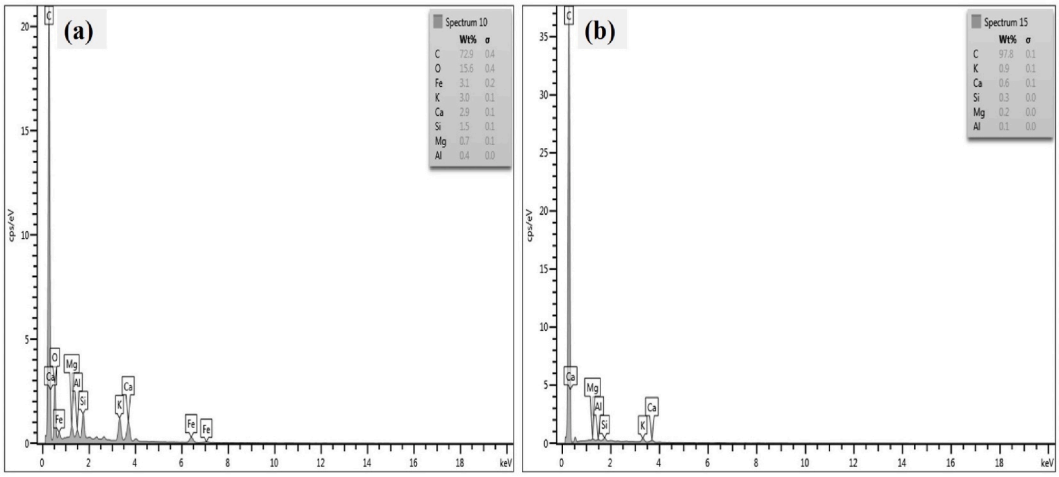

Figure [8]. EDX (a) AC/Fe before growth and (b) after growth for O-CNT.

Table 3
BET surface area, pore volume, and pore volume for all absorbents.

Adsorbent	BET surface area (m^2/g)	Pore volume (cc/g)	Pore diameter (nm)
I-PAC	669.72	0.312	1.53
O-PAC	1092.342	0.598	2
I-CNT	71.42	0.230	12
O-CNT	54.26	0.156	11

Fig. [5b]. Therefore, the contribution of Fe catalyst is 2.9%, followed by Si, Ca, Al, and Mg at <3%, O at 10.5% and C at 76.7%. Moreover, CNTs are noticed, where successful grown-up on surface of I-PAC for C 98.4%. Due to reaction process, the other elements are dissipated as illustrated in Fig. [5d].

Moreover, to investigate and confirm the growth of CNTs, TEM is illustrated in Fig. [6], where they have revealed the internal surface structure for I-CNT on I-PAC to refer for fine quality of CNTs. Therefore, dark spots represent metallic clusters of catalyst where C atom builds up the structure of CNTs.

The structures and morphologies of prepared O-CNT are captured through FESEM prior to and after synthesis. Fig. [7(a, b)] demonstrates FESEM of varied magnifications to be noticed before growth (AC/Fe). The catalyst is dispersed and surface of substrate is rough. Fig. [7(c, d)] reveals that a carpet-like deposit including highly dense O-CNT arrays without proved catalyst impurities after growth is available. The nanotube's diameter is about 34.18 nm–37.45 nm. TEM confirms O-CNT has a structure of high quality (Fig. [7 (e, f)]). The grain size using FESEM is more reliable than utilizing equation [4].

EDX has detected the elements of substrate prior and after the growth. Fig. [8a] illustrates EDX spectra to refer for successful embedded catalyst on AC/Fe surface. The O-CNT's surface includes 97.8% C after growth with impurities disappeared Fe and O after increased high temperature, whereas other elements such as K, Ca, Si, Mg, and Al decreased by less than 1 wt%. as shown in Fig. [8b].

The date palm fiber-based low-cost carbon nanotubes (CNTs) and nanostructured powder activated carbon (DP-NPAC) have been investigated to regenerate and reusable materials for finding that they could be effectively regenerated and reused multiple times, making them a cost-effective and sustainable solution for CNTs production in various application. Overall, the DP-NPAC and CNTs synthesized in this study have demonstrated promising applications in multi-application. The Brunauer-Emmett-Teller (BET) surface area, pore-volume and pore size of DP-NPAC and CNTs have been investigated by our group as shown in Table 3 [23–26] and pointing to possible directions for future development [27–38].

4. Conclusions

It is concluded that date palm fiber-based low-cost carbon nanotubes (CNTs) and nanostructured powder activated carbon (DP-NPAC) were synthesized. The results have showed that both I-CNT and O-CNT have a high capacity, with CNTs exhibiting a slightly higher capacity than I-PAC and O-PAC. The structural characterization of materials, which included techniques such as FESEM, TEM and XRD have provided a valuable information on their surface morphology and structural features. The results have showed that both I-CNT and O-CNT have a high surface area and a porous structure, which contributed to their excellent functions. These materials could be used in various applications, including water treatment and environmental remediation.

Funding

No funding was received.

Author contribution statement

Alfarooq O. Basheer: Conceived and designed the experiments; Performed the experiments;
Ali Abu Odeh: Contributed reagents, materials, analysis tools or data;
Y. Al-Douri: Analyzed and interpreted the data; Wrote the paper.

Data availability statement

No data was used for the research described in the article.

Declaration of competing interest

The authors declare that they have no known competing financial interests or personal relationships that could have appeared to influence the work reported in this paper.

Appendix A. Supplementary data

Supplementary data to this article can be found online at https://doi.org/10.1016/j.heliyon.2023.e18811.

References

[1] Muhammad Aqeel Ashraf, S. Khaled, Balkhair, ahmed jalal khan chowdhury, marlia mohd hanafiah, treatment of taman beringin landfill leachate using the column technique, Desalination Water Treat. 149 (2019) 370–387.
[2] M. Mishra, M. Chauhan, Biosorption as a novel approach for removing aluminium from water treatment plant residual—a review, in: Water Quality Management, Springer, 2018, pp. 93–99.
[3] S.A. Al-Muhtaseb, M.H. El-Naas, S. Abdallah, Removal of aluminum from aqueous solutions by adsorption on date-pit and BDH activated carbons, J. Hazard Mater. 158 (2008) 300–307.
[4] A. Abbas, Al-Raad, Marlia M. Hanafiah, Ahmed Samir Naje, Ajeel Mohammed A, Basheer Alfarooq O, Thuraya Ali Aljayashi, Mohd Ekhwan Toriman, Treatment of saline water using electrocoagulation with combined electrical connection of electrodes, Processes 7 (2019) 242–251.
[5] Mohammad Al-Harahsheh, Marwan Batiha, Sami Kraishan, Habis Al-Zoubi, Precipitation treatment of effluent acidic wastewater from phosphate-containing fertilizer industry: characterization of solid and liquid products, Separ. Purif. Technol. 123 (2014) 190–199.
[6] J. Shen, A. Schäfer, Removal of fluoride and uranium by nanofiltration and reverse osmosis: a review, Chemosphere 117 (2014) 679–691.
[7] C.S. Lee, J. Robinson, M.F. Chong, A review on application of flocculants in wastewater treatment, Process Saf. Environ. Protect. 92 (2014) 489–508.
[8] H. Yuan, Z. He, Integrating membrane filtration into bioelectrochemical systems as next generation energy-efficient wastewater treatment technologies for water reclamation: a review, Bioresour. Technol. 195 (2015) 202–209.
[9] Xinyue Gao, Chang'an Wang, Wengang Bai, Yujie Hou, Defu Che, Experimental investigation of the catalyst-free reaction characteristics of micron aluminum powder with water at low and medium temperatures, J. Energy Storage 59 (2023) 106543–106559.
[10] Yufeng Da, Yong Liu, Yong Chen, Rui Han, Jianlong Wang, Promotion of O2 activation by ZIF-8 derived N-rich aluminum-graphite (Al-Gr-NPC) composite for non-radical degradation of antibiotic at neutral pH, Separ. Purif. Technol. 308 (2023) 122806–122812.
[11] M.R. Morovvati, B. Mollaei-Dariani, A. Lalehpour, D. Toghraie, Fabrication and finite element simulation of aluminum/carbon nanotubes sheet reinforced with Thermal Chemical Vapor Deposition (TCVD), J. Mater. Res. Technol. 23 (2023) 1887–1902.
[12] Qiang Liu, Junli Wang, Wenshuai Liu, Taleeb Zedan Taban, Mustafa M. Kadhim, A. Sarkar, Thermodynamic and density functional theory study the removal of different forms of gas arsenic by using aluminum nitride nanotube, Fuel 329 (2022) 125395–125404.
[13] U. Moralı, H. Demiral, S. Şensöz, Optimization of activated carbon production from sunflower seed extracted meal: taguchi design of experiment approach and analysis of variance, J. Clean. Prod. 189 (2018) 602–611.
[14] M. Poletto, H.L. Ornaghi, A.J. Zattera, Native cellulose: structure, characterization and thermal properties, Materials 7 (2014) 6105–6119.
[15] A. Zubrik, Marek Matik, Slavomír Hredzák, Michal Lovás, Zuzana Danková, Milota Kováčová, Jaroslv Briančin, Preparation of chemically activated carbon from waste biomass by single-stage and two-stage pyrolysis, J. Clean. Prod. 143 (2017) 643–653.
[16] Yuhong Kang, Xianyong Wei, Guanghui Liu, Miao Mu, Xiangrong Ma, Yong Gao, Zhimin Zong, CO2-hierarchical activated carbon prepared from coal gasification residue: adsorption equilibrium, isotherm, kinetic and thermodynamic studies for methylene blue removal, Chin. J. Chem. Eng. 28 (2020) 1694–1700.
[17] B. Hameed, I. Tan, A. Ahmad, Preparation of oil palm empty fruit bunch-based activated carbon for removal of 2, 4, 6-trichlorophenol: optimization using response surface methodology, J. Hazard Mater. 164 (2009) 1316–1324.
[18] K. Foo, B. Hameed, Preparation and characterization of activated carbon from pistachio nut shells via microwave-induced chemical activation, Biomass Bioenergy 35 (2011) 3257–3261.
[19] Josphat Phiri, Jinze Dou, Tapani Vuorinen, A. Patrick, C. Gane, Thaddeus C. Maloney, Highly porous willow wood-derived activated carbon for high-performance supercapacitor electrodes, ACS Omega 4 (2019) 18108–18117.
[20] Asma Nasrullah, A.H. Bhat, Abdul Naeem, Isa Mohamed Hasnain, Danish Mohammed, High surface area mesoporous activated carbon-alginate beads for efficient removal of methylene blue, Int. J. Biol. Macromol. 107 (2018) 1792–1799.
[21] V.E. Pakade, N.T. Tavengwa, L.M. Madikizela, Recent advances in hexavalent chromium removal from aqueous solutions by adsorptive methods, RSC Adv. 9 (2019) 26142–26164.
[22] S. Boscarino, S. Filice, A. Sciuto, S. Libertino, M. Scuderi, C. Galati, S. Scalese, Investigation of ZnO-decorated CNTs for UV light detection applications, Nanomaterials 9 (2019) 1099–1109.

[23] Alfarooq O. Basheer, Marlia Mohd Hanafiah, Alsaadi Mohammed Abdulhakim, Y. Al-Douri, M.A. Malek, Mustafa Mohammed Aljumaily, Seef Saadi Fiyadh "Synthesis and characterization of natural extracted precursor date palm fibre-based activated carbon for Aluminium removal by, RSM optimization" processes 7 (2019) 249–268.
[24] Alfarooq O. Basheer, Marlia Mohd Hanafiah, Mohammed Alsaadi, W.Y. Wan Zuhairi, Y. Al-Douri, "Synthesis, characterization and analysis of hybrid carbon nanotubes by chemical vapor deposition, Application for Aluminium removal" polymers 12 (2020) 1305–1322.
[25] Alfarooq O. Basheer, Marlia M. Hanafiah, Alsaadi Mohammed Abdulhakim, W. Wan Zuhairi, Y. Y, A. Al-Douri, Bouhemadou "Synthesis and characterization of low-cost carbon nanotubes by chemical vapor deposition for Aluminium removal from aqueous solution" Desalination and Water, Treatment 214 (2021) 440–451.
[26] Alfarooq O. Basheer, Marlia M. Hanafiah, Y. Mohammed Abdulhakim Alsaadi, Al-Douri, A. Abbas, Al-Raad "Synthesis and optimization of high surface area mesoporous date palm fiber-based nanostructured powder activated carbon for Aluminium removal" Chinese, J. Chem. Eng. 32 (2021) 472–484.
[27] D. Paul, Fretting wear behavior of aluminum coatings" Experimental and Theoretical NANOTECHNOLOGY 7 (2023) 257–267.
[28] J. Fuji, T. Shuji, F. Jumbo, G. Saraki, M. Tanemura, Optical analysis of multi-crystalline Si surface" Experimental and Theoretical NANOTECHNOLOGY 7 (2023) 273–282.
[29] M.C. Paşal, C.M. Aras, Investigation of semi-metallic properties of GdS band TbSb compounds" Experimental and Theoretical, Nanotechnology 7 (2023) 371–380.
[30] Oula Jabbar, H. Ali, Reshak "Structural, electronic, and optoelectronic properties of XYZ2 (X=Zn,Cd; Y=Si,Sn;Z=pnicogens) Chalcopyrite compounds, First-principles calculations" Experimental and Theoretical NANOTECHNOLOGY 7 (2023) 97–110.
[31] L. Li, S. Naher, Half-metallic behavior Co2YAl (Y= Mo,Tc), compounds" Experimental and Theoretical NANOTECHNOLOGY 7 (2023) 127–138.
[32] J. Christ, M. Filips, S. Artois, R. Nowak, M. Reed, W. Knoll, Sliding wear of rubber/layered silicate nanocomposites" Experimental and Theoretical NANOTECHNOLOGY 7 (2023) 159–170.
[33] M. Al-Jassim, G. Grüner, J. Guo, "GaN on Si (111) nanostructure for solar cells application" Experimental and Theoretical NANOTECHNOLOGY 6 (2022) 447–452.
[34] C. Felser, S. Kaskel, A. Rubio, Surface ion with Mo, Ti and Al for steel studies" Experimental and Theoretical NANOTECHNOLOGY 6 (2022) 477–484.
[35] Surbhi Sharma "In-doped Aluminum antimonide alloy for optoelectronic applications" Experimental and, Theoretical NANOTECHNOLOGY 6 (2022) 295–316.
[36] S. Alex, Micro-size Aluminum for environmental detonation" Experimental and Theoretical NANOTECHNOLOGY 6 (2022) 333–345.
[37] Osama ismail "analysis of localized corrosion on stainless, Steel" Experimental and Theoretical NANOTECHNOLOGY 6 (2022) 209–222.
[38] M. Sealen, O. Engstrom, Morphological studies of Si nanowires effect on the photovoltaics" Experimental and Theoretical, Nanotechnology 6 (2022) 53–60.